T 1217

DIGITAL RESTORATION OF STRAIN STEPS FROM STRAIN-METER TRANSIENTS

by

Ninos B. Benyamin

ProQuest LLC.
789 East Eisenhower Parkway
P.O. Box 1346
Ann Arbor, MI 48106 – 1346

T 1217

A thesis submitted to the Faculty and the Board of Trustees of the Colorado School of Mines in partial fulfillment of the requirements for the degree of Master of Science.

Signed: Ninos Benyamin
Ninos Benyamin

Golden, Colorado
Date: 20 Sept., 1968

Approved: Frank Hadsell
Dr. F. Hadsell
Thesis Advisor

Prof. J. C. Hollister
Head of Department

Golden, Colorado
Date: 20 Sept, 1968

ABSTRACT

This paper further confirms the existence of propagating strain steps which are detectable at large epicentral distances. An inverse digital filter is designed to process strain-seismograph transient records. For this study the signal is in the low-frequency spectrum which is severely attenuated by the RC recording filter, and the noise refers, for the most part, to crustal surface waves. This classification is the result of an analysis of the sampled data and the characteristics of the recording system.

By the application of the operator to the strain-meter record of a California earthquake (recorded in Colorado in 1966), a good low-pass representation of a propagating elastic step is recovered. From the argument (phase) of the Fourier transform of the transient record, the arrival time of the step component of the transient is also computed.

TABLE OF CONTENTS

LIST OF FIGURES

ACKNOWLEDGMENTS

The author wishes to express his appreciation to Dr. Frank Hadsell for his guidance and valuable suggestions, and to Dr. Maurice Major for his helpful comments throughout the writing.

I am indebted to Dr. Russell L. Gray for the use of his several program suites.

I would also like to thank Mr. David Butler and Mr. Philip Romig, who have contributed in one way or another to the writing of this paper.

My special thanks go to my wife, Annette, whose encouragement and patience made the task possible.

INTRODUCTION

In the past few years a number of propagating elastic disturbances have been observed on strain-meter records (Benioff, 1963) and have been associated with hypothetical propagating strain steps in the strain field of the earth (Wideman, 1967). However, there is some question about the possibility of detecting permanent strain steps for large epicentral distances. The causes for concern are (a) it has been suggested that most strain meters have been built following H. Benioff's design and because these instruments are extremely sensitive, it is plausible that they will undergo a permanent mechanical or electrical offset after a large earthquake (Major, 1966, p. 31); (b) artificially induced strains have failed to show a permanent strain offset; and (c) some theoretical predictions suggest that the steady-state strains vary with distance like R^{-2} (Pekeris, 1955) or R^{-3} (Press, 1965). Such decay of amplitude with distance will produce strains which are below the sensitivity range of modern instruments.

Press (1965) takes the position that these events are real and that they are not the result of an instrumental defect. He bases his argument on the fact that the strain offsets are consistent with the predictions of dislocation

theory (Press, 1965, p. 2406). For the field proof he cites the earthquake of Nãnã, Peru. This earthquake was recorded on two identical strain meters at right angles to each other. One strain meter showed a distinct residual strain, whereas the other did not.

Wideman (1967) introduces further evidence to support the reality of the step components of the propagating elastic disturbances. His argument rests on (a) the observation that strain-step amplitude is dependent upon earthquake magnitude and epicentral distance over a wide range of magnitudes and distances, (b) an excellent fit of the empirical step response of the strain meter with the seismograms, (c) the fact that strain steps have nearly constant speed of propagation over a wide range of epicentral distances and hence resemble surface waves, and (d) they occur after the arrival of Rayleigh waves as predicted by Pekeris (1955, p. 480).

In this paper the following accomplishments are described:

> A digital filter is designed to recover relatively low frequencies (120- to 90,000- second period) attenuated by the RC filter of the seismograph. Here, relatively high-frequency noise (5- to 40-second period) imposed the principal design constraint.
>
> By the application of the digital filter to the transient record, a good low-pass representation of a propagating elastic step is recovered.

From the argument (phase) of the Fourier transform of the data (strain seismograph output), the arrival time of the strain step is computed.

The computer centers of Colorado School of Mines and National Bureau of Standards, Boulder, Colorado, were used throughout the project. All the computer programs and numerical results may be obtained from Dr. Frank Hadsell, Geophysics Department, Colorado School of Mines.

FREQUENCY RESPONSE OF THE RECORDING SYSTEM

A schematic diagram of the recording system of the strain meter is shown in Figure 1. Its design, except for a few modifications, is essentially that of Major et al (1964). Dual recording and filtering of the transducer output is desirable to enhance the dynamic range of the system. The circuit consists of a T and a π section in tandem separated from another T and a shunt section by a Hewlett-Packard (425A) d-c amplifier.

In addition to providing voltage amplification (usually run at 100; ie., $V_3 = 100V_2$), the amplifier also provides an impedance match between the transducer and seismic recorder. Specifications of the amplifier indicate that it has a flat amplitude and zero phase response up to about 3 seconds. The 0.5 megaohm internal impedance of the transducer was measured by means of the variable load technique by Mr. Romig (personal communication). Because the series impedance of the source is small compared with the overall impedance of the circuit, the transducer can be considered as an ideal voltage source. Inasmuch as V_2 is applied to the grid of the amplifier's vacuum tube, the input impedance of the d-c amplifier can be taken to be infinite. The input impedances of seismic and tide recorder, under balanced conditions, can also be considered infinite. (Balance time is approximately

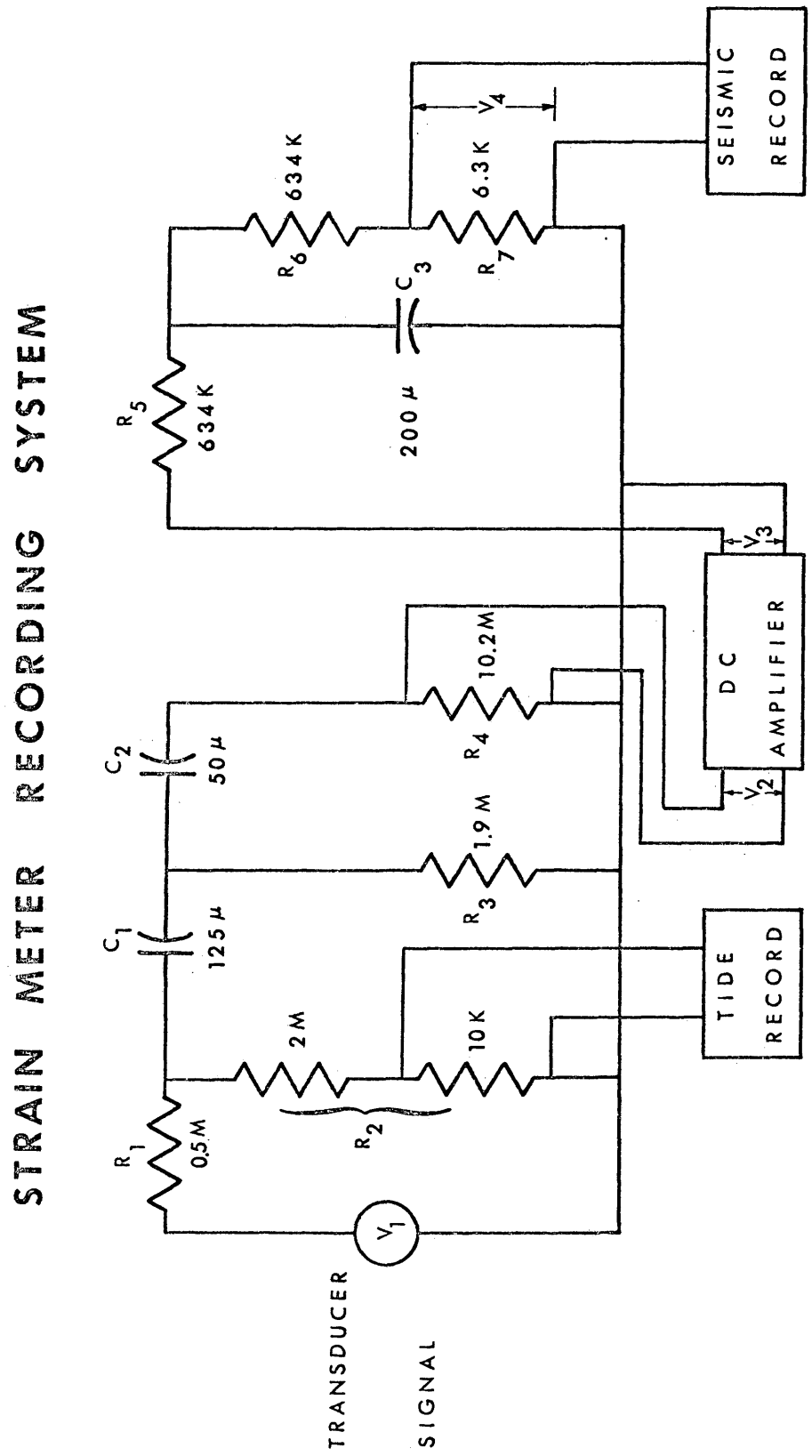
STRAIN METER RECORDING SYSTEM
TRANSDUCER SIGNAL
V_1
R_1 0.5M
R_2 2M 10K
C_1 125 μ
R_3 1.9 M
C_2 50 μ
R_4 10.2M
V_2
DC AMPLIFIER
V_3
TIDE RECORD
R_5 634 K
C_3 200 μ
R_6 634 K
R_7 6.3 K
V_4
SEISMIC RECORD

Figure 1

0.1 second.) The amplifier behaves as an isolation box in view of the fact that the frequencies of interest are below 3 seconds. From the foregoing, we can write the system function of the entire circuit as

$$W(s) = K.\ W_1.\ W_2 = 100(V_2/V_1).(V_4/V_3),$$

where K is the system function of the d-c amplifier.

In the circuit of Figure 1 each section is a four-terminal network. Pipes (1958, p. 183) shows that for a four-terminal network with V_1, I_1 as inputs and V_2 and I_2 as outputs, a linear relationship exists between the above quantities. This relationship is usually given in terms of a 2 by 2 matrix called transmission matrix as

$$\begin{bmatrix} V_1 \\ I_1 \end{bmatrix} = \begin{bmatrix} A & B \\ C & D \end{bmatrix} \begin{bmatrix} V_2 \\ I_2 \end{bmatrix}.$$

It can be shown that the determinant of the matrix is unity; ie.,

$$AD - BC = 1.$$

The restrictions on the component elements of the network are that they be linear, constant, and passive. Table 1 gives the transmission matrices of the three types of network which appear in the calculations.

TABLE 1

Network	Transmission Matrix $\left[T\right]=\begin{bmatrix} A & B \\ C & D \end{bmatrix}$
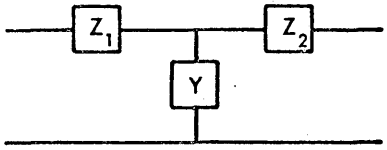 T section	$\begin{bmatrix} 1+YZ_1 & Z_1+Z_2+YZ_1Z_2 \\ Y & 1+YZ_2 \end{bmatrix}$
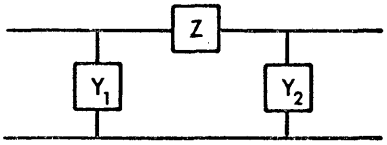 π section	$\begin{bmatrix} 1+ZY_2 & Z \\ Y_1+Y_2+ZY_1Y_2 & 1+ZY_1 \end{bmatrix}$
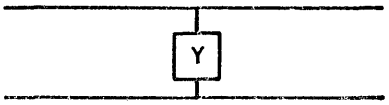 Shunt section	$\begin{bmatrix} 1 & 0 \\ Y & 1 \end{bmatrix}$

(after Pipes, 1958, p. 185)

The function $W_1(s)$ is given by $W_1(s) = V_2/V_1$ where V_1 and V_2 are obtained from

$$\begin{bmatrix} V_1 \\ I_1 \end{bmatrix} = \left[T\right]_1 \left[T\right]_2 \begin{bmatrix} V_2 \\ I_2 \end{bmatrix} = \begin{bmatrix} A & B \\ C & D \end{bmatrix} \begin{bmatrix} V_2 \\ I_2 \end{bmatrix}$$

Here, $\left[T\right]_1$ and $\left[T\right]_2$ are the transmission matrices of the T and π sections, respectively. Since the input impedance of the d-c amplifier is infinite, ie., $I_2 = 0$, we have

$$\frac{V_2}{V_1} = \frac{1}{A} \quad .$$

The component A is obtained from $[T]_1$ $[T]_2$ where

$$[T]_1[T]_2 = \begin{bmatrix} 1+\frac{R_1}{R_2} , R_1+\frac{1}{C_1S}+\frac{R_1}{R_2C_1S} \\ \frac{1}{R_2} , 1+\frac{1}{R_2C_1S} \end{bmatrix}$$

$$\begin{bmatrix} 1+\frac{1}{C_2R_4S} , \frac{1}{C_2S} \\ \frac{1}{R_3}+\frac{1}{R_4}+\frac{1}{R_3R_4C_2S} , 1+\frac{1}{R_3C_2S} \end{bmatrix}$$

which after matrix multiplication and numerical substitution (refer to Figure 1) becomes

$$\frac{1}{A} = \frac{2.43 \times 10^5 \, S^2}{2.5\ (667S+1)(227S+1)} \quad .$$

Similarly, $W_2 = V_4/V_3$ where

$$\begin{bmatrix} V_3 \\ I_3 \end{bmatrix} = [T]_3[T]_4\begin{bmatrix} V_4 \\ I_4 \end{bmatrix} = \begin{bmatrix} A' & B' \\ C' & D' \end{bmatrix}\begin{bmatrix} V_4 \\ I_4 \end{bmatrix}$$

and $[T]_3$ and $[T]_4$ are the transmission matrices of the T and shunt sections in tandem with the amplifier. Again since $I_4 = 0$, we have

$$\frac{V_4}{V_3} = \frac{1}{A'} \quad .$$

Hence, we have

$$[T]_3[T]_4 = \begin{bmatrix} 1+R_5C_3S , R_5+R_6+R_5R_6C_3S \\ C_3S , 1+R_6C_3S \end{bmatrix}\begin{bmatrix} 1 & 0 \\ \frac{1}{R_7} & 1 \end{bmatrix}$$

from which we obtain

$$\frac{1}{A'} = \frac{1}{200(63.4\ S+1)} \quad .$$

Finally,

$$W(s) = 100(V_2/V_1)(V_4/V_3) = \frac{100}{A\ A'}$$

or

$$W(s) = \frac{4.86 \times 10^4\ S^2}{(667S+1)(227S+1)(63.4S+1)} \qquad \text{eq. 1}$$

The pole-zero diagram corresponding to the system function is shown in Figure 2, as follows:

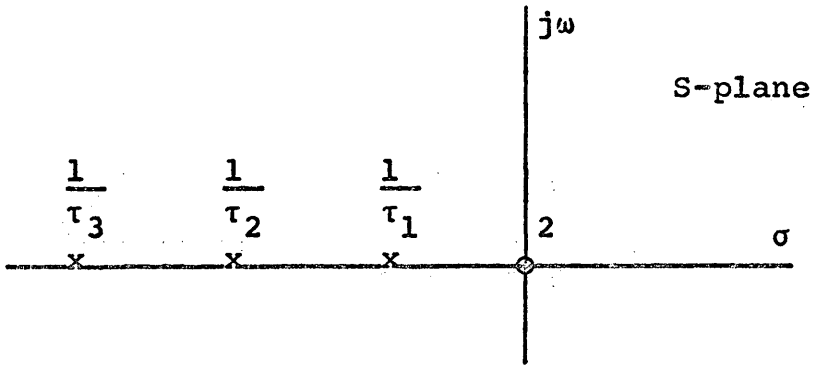

Figure 2. Pole-Zero Diagram of the RC Recording Filter.

where $\frac{1}{\tau_1} = -1.5\text{x}10^{-3}$ rad/sec, $\frac{1}{\tau_2} = -4.4\text{x}10^{-3}$ rad/sec, and $\frac{1}{\tau_3} = -15.8\text{x}10^{-3}$ rad/sec.

The Fourier transform of the system's impulse response, $W(\omega)$, is by definition the frequency response. For causal systems, such as the filter under study, $w(t) = 0$ for $t < 0$

and the bilateral Laplace transform equals the unilateral Laplace transform; and if the Fourier transform exists, we have

$$W_{II}(j\omega) = W_{I}(j\omega) = W(\omega).$$

The function $W(\omega)$ is complex and can be represented as $W(\omega) = |W(\omega)|e^{j\phi(\omega)}$ where $|W(\omega)|$ is the amplitude and $\phi(\omega)$ the phase response. The amplitude and phase responses were plotted by means of Bode diagrams (Aseltine, 1958, p. 143). The graphs consist of a plot of 20 log $|W(\omega)|$ vs log ω and another plot of arg $W(\omega)$ vs log ω. The graphs are shown in figures 3 and 4.

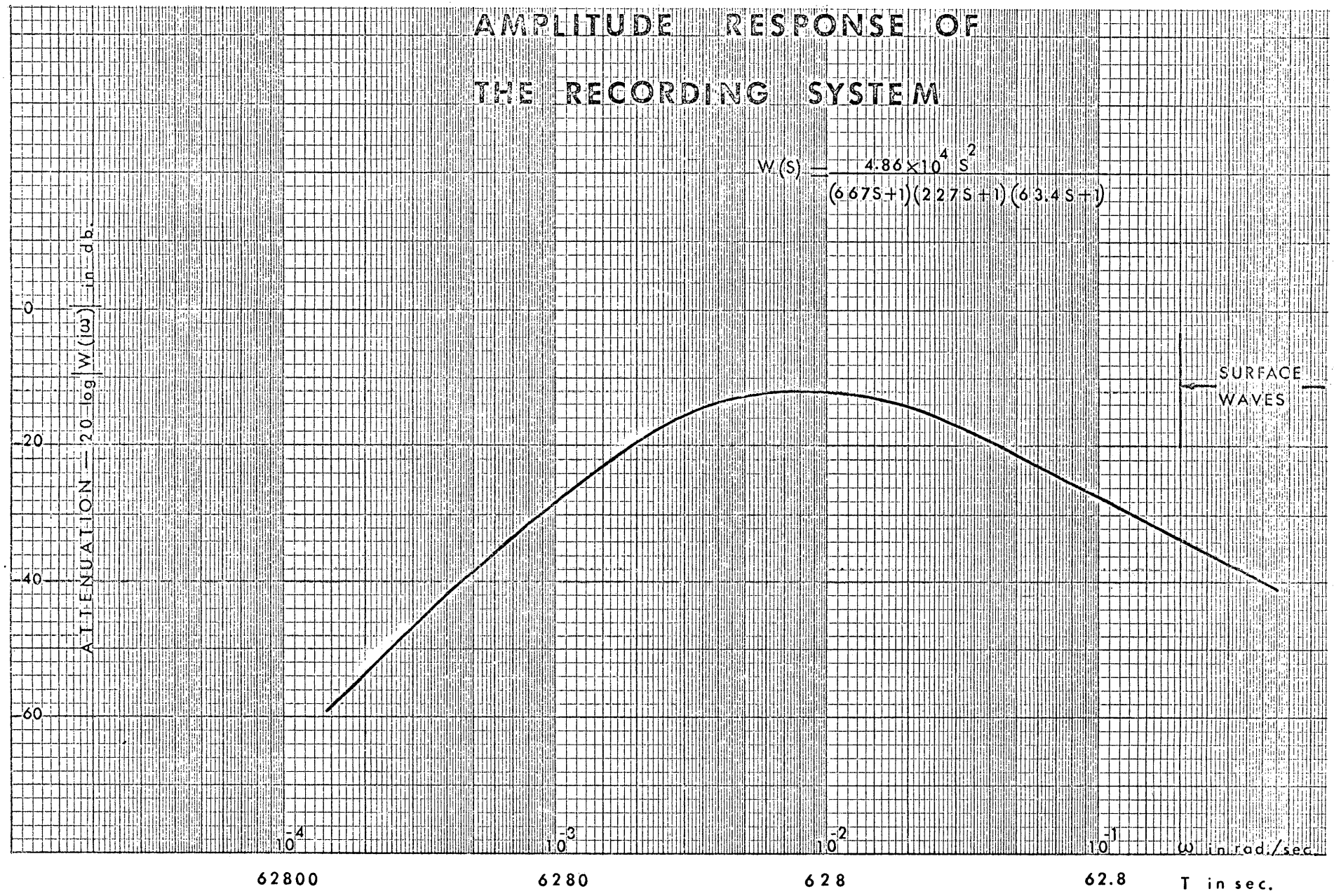
AMPLITUDE RESPONSE OF
THE RECORDING SYSTEM
$W(S) = \frac{4.86 \times 10^4 S^2}{(667S+1)(227S+1)(63.4S+1)}$
ATTENUATION — 20 log |W(iω)| in db.
0
-20
-40
-60
SURFACE WAVES
10^{-4}
10^{-3}
10^{-2}
10^{-1}
ω in rad./sec.
62800
6280
628
62.8
T in sec.

Figure 3

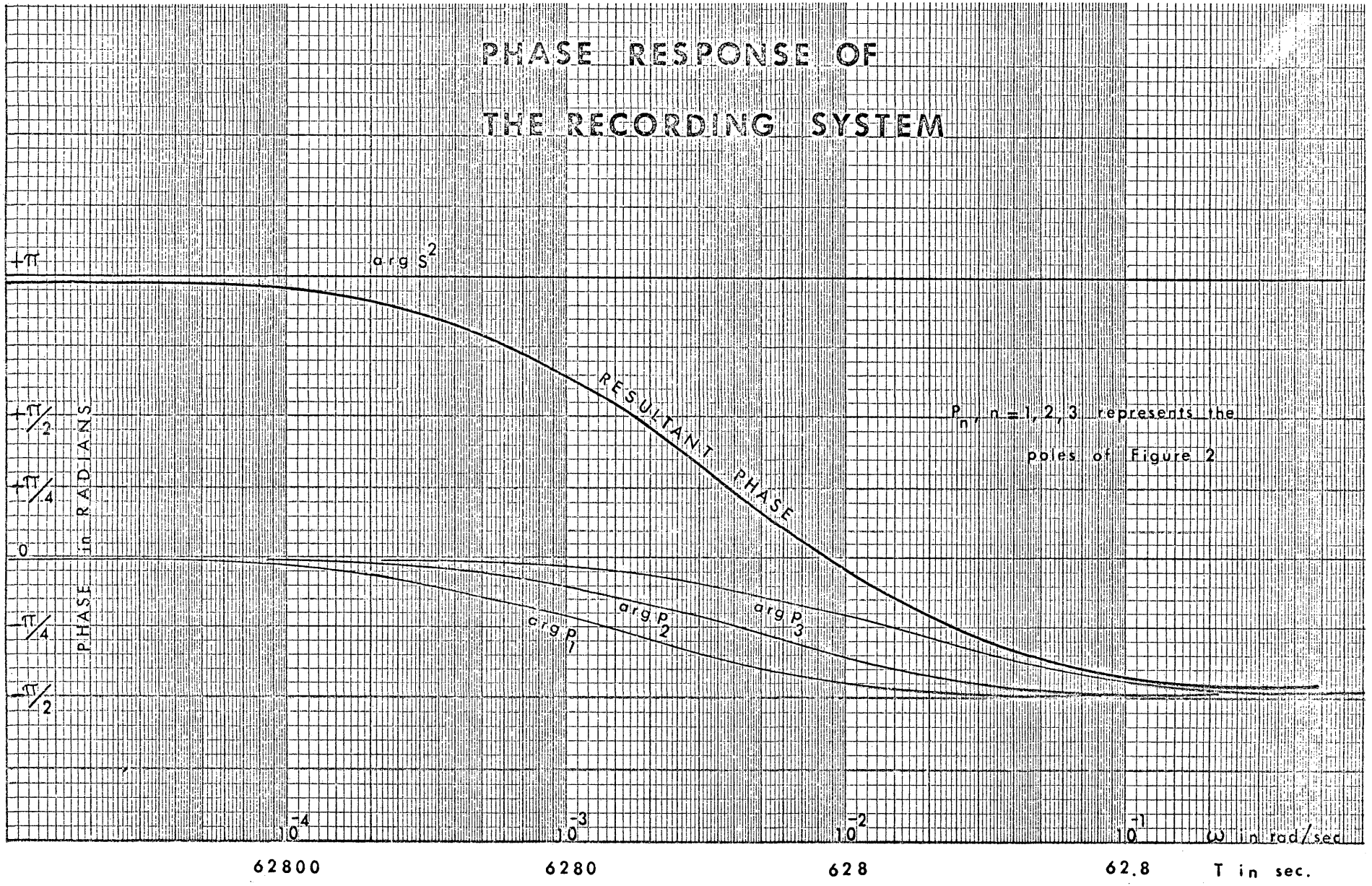
PHASE RESPONSE OF
THE RECORDING SYSTEM
+π
arg S²
+π/2
+π/4
0
-π/4
-π/2
PHASE in RADIANS
RESULTANT PHASE
Pn, n = 1, 2, 3 represents the
poles of Figure 2
arg P1
arg P2
arg P3
10⁻⁴
10⁻³
10⁻²
10⁻¹
ω in rad/sec
62800
6280
628
62.8
T in sec.

Figure 4

ANALYSIS OF THE DATA

The data used in this study was the output of a strain seismograph with an amplitude response as shown in Figure 3. The strain meter is installed in the Cecil H. Green Observatory at Bergen Park, Colorado, which is about 25 miles southwest of downtown Denver. The earthquake that caused the disturbance occurred on September 12, 1966, in Northern California. The magnitude was about 6 (Richter scale), and the epicentral distance was 1246 km. The filtered record is shown in the upper portion of Figure 16.

This section is discussed under the following headings:

Sampling of the Data

Fourier Transform of the Sampled Data

Sampling of the Data

For the purpose of digital processing, the seismic record was sampled. The method of sampling was rather simple. The data was projected on cross-section paper, and the screen to projector distance was adjusted until the required number of intervals were formed in one minute. In the process the record was magnified many times, but there was also some optical distortion which caused a gradual increase of minute intervals. This increase amounted to 20 seconds for a total of 15 minutes of digitized record. The error is ignored in

this study.

A 2-second sampling interval was used. The choice was based on the visual examination of the frequency content of the record as well as the degree of aliasing (Hadsell, 1968, p. 51) introduced at this sampling rate. The percent aliasing was computed from the amplitude response of the filter. The 6 db-per-octave slope of Figure 3 was extended to higher frequencies, as is shown in Figure 5. The Nyquist period, $1/f_N$, is 4 seconds. The percent aliasing at the frequency $f_N-\gamma$ is defined by

$$\text{percent aliasing at } f_N-\gamma = \frac{A(f_N+\gamma)}{A(f_N-\gamma)} \times 100.$$

For $\frac{1}{f_N-\gamma} = 31$ seconds, the percent aliasing is

$$\frac{1.26 \times 10^{-3}}{2 \times 10^{-2}} \times 100 = 6.3.$$

This degree of aliasing may seem alarming. However, we should remember that this component of the surface waves is the upper limit of the spectrum of interest. Similarly, the 100-second aliasing can be shown to be only 1.8 percent.

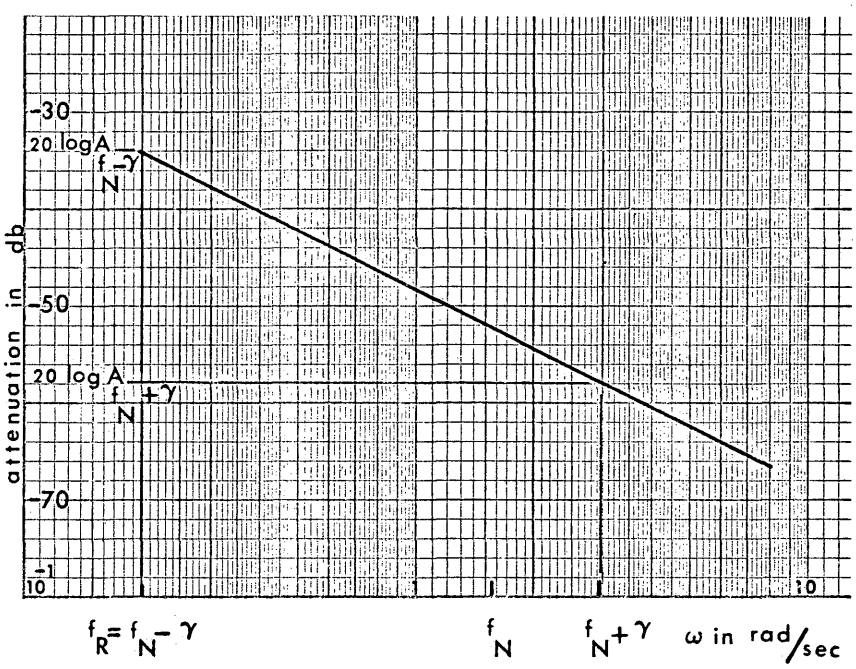

Figure 5. High-Cut Branch of the RC Filter.

Fourier Transform of the Sampled Data

A Fourier transform of the data was run in order to study the amplitude and phase of the sampled data (program no. 2, see the introduction). The results are shown in Figure 6. Prior to this, the program was tested (program no. 1-a and 1-b).

The amplitude curve indicates that the data are relatively rich in the low frequencies; however the extremely low frequencies, which are essential building blocks of any event such as a strain step, are attenuated. This feature is in agreement with the amplitude response of the RC filter.

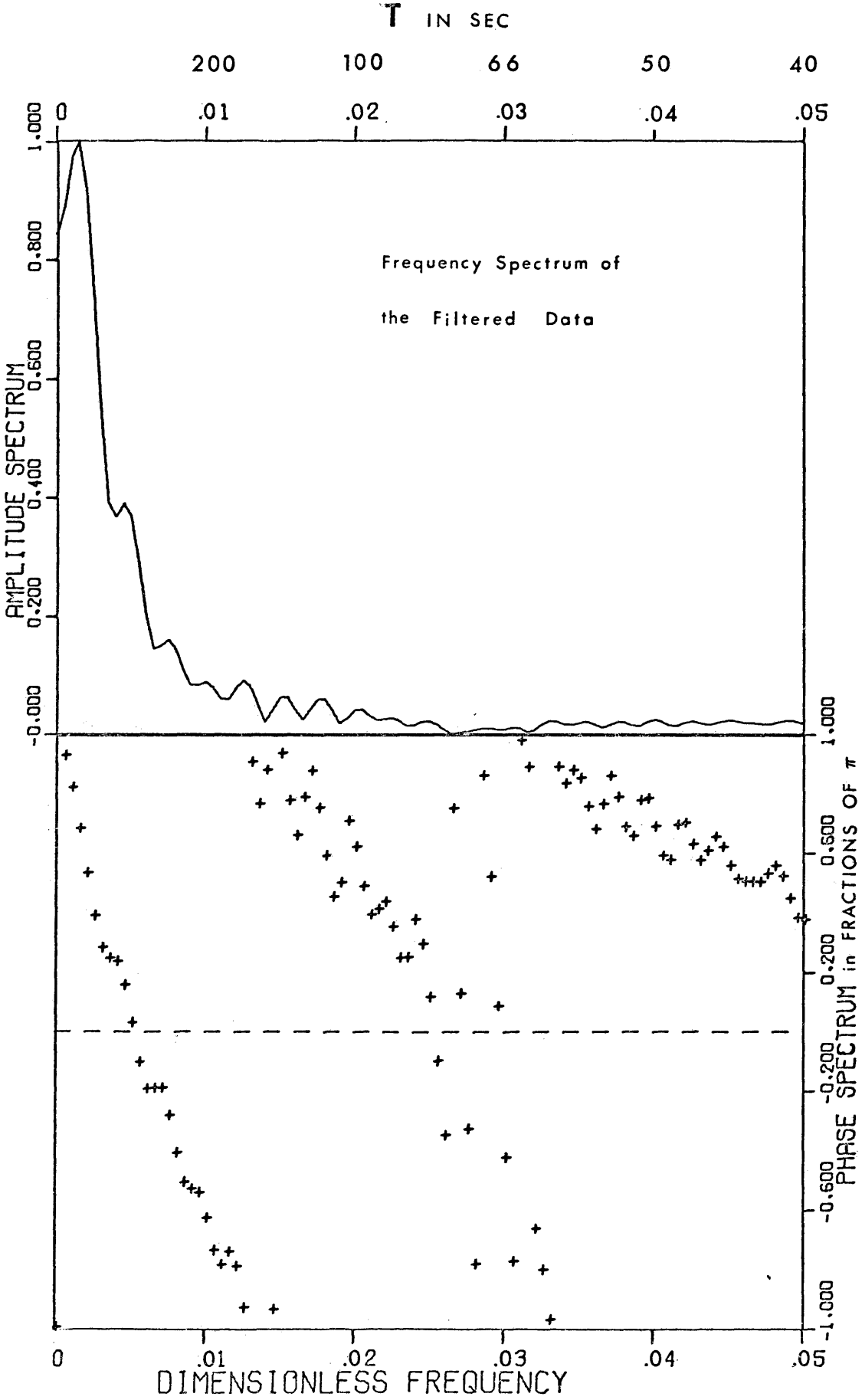
T IN SEC
200
100
66
50
40
0
.01
.02
.03
.04
.05
Frequency Spectrum of
the Filtered Data
AMPLITUDE SPECTRUM
1.000
0.800
0.600
0.400
0.200
-0.000
PHASE SPECTRUM in FRACTIONS OF π
1.000
0.600
0.200
-0.200
-0.600
-1.000
DIMENSIONLESS FREQUENCY

Figure 6

It must be mentioned that the d-c amplitude in the graph is not reliable, as it depends on the choice of zero line in the original data. If the exact zero line was known and used, the d-c component would have been zero.

The periodic peaks are, almost certainly, the result of truncation of the data. To see this we recall that the transform of a truncated and digitized data is given as

$$f(t)\cdot\sum_{n=0}^{N}\delta(t-n\Delta t)\longleftrightarrow\frac{1}{2\pi}\{F(\omega)*\frac{\mathrm{Sin}(N+\frac{1}{2})\omega\Delta t}{\mathrm{Sin}(\omega\Delta T/2)}\}$$

where $f(t)$ is the continuous data, $F(\omega)$ its Fourier transform, and the term $\mathrm{Sin}(N+\frac{1}{2})\omega\Delta T/\mathrm{Sin}(\omega\Delta T/2)$ is called the Fourier-Series kernel. It can be shown (Gray, 1965, p. 95) that the first small peak of the kernel arrives, approximately, $(f\Delta T)_1$ units after the main peak where

$$(f\Delta T)_1\simeq\frac{5}{2}\,(1/2N+1) = 2.78\times10^{-3},\ N = 451.$$

The following successive peaks appear $(f\Delta T)_2$ units after the first small peak where

$$(f\Delta T)_2\simeq2(1/2N+1) = 2.15\times10^{-3}.$$

The corresponding intervals as measured from Figure 6 are 3.2×10^{-3} and 2.5×10^{-3} respectively. This close check suggests that the peaks are caused by truncation of the data.

The striking feature of the graph is the almost linear phase curve. The deviation from a straight line was caused, as supported by Figure 4, by the nonlinear phase contamination of the RC filter. In Figure 7 the phase distortion was

accounted for, and the outcome is a straight line. The significance of this finding will become apparent after a brief review of the mathematical background. The Fourier transform pairs are formally defined as

$$F(\omega) = \int_{-\infty}^{\infty} f(t) e^{-j\omega t} dt$$

and

$$f(t) = \frac{1}{2\pi} \int_{-\infty}^{\infty} F(\omega) e^{j\omega t} d\omega$$

or

$$f(t) \Longleftrightarrow F(\omega) .$$

If the function f(t) is delayed an amount t_o, then its amplitude spectrum remains the same; but a linear term $-t_o\omega$, with negative slope, is added to its phase angle (Papoulis, 1962, p. 14); ie.,

$$f(t-t_o) \Longleftrightarrow F(\omega) e^{-j\omega t_o} = A(\omega) e^{j\{\phi(\omega) - t_o\omega\}} .$$

At this stage we can observe that in the frequency band 0.001 to 0.02, the resultant phase of Figure 7 is consistent with a propagating elastic disturbance of the type shown in Figure 8. Here, component B carries most of the energy in the above frequency band. Inasmuch as component B has a constant phase (see Figure 9), it follows that the linear feature of the phase in Figure 7 is indicative of a shift in the time domain.

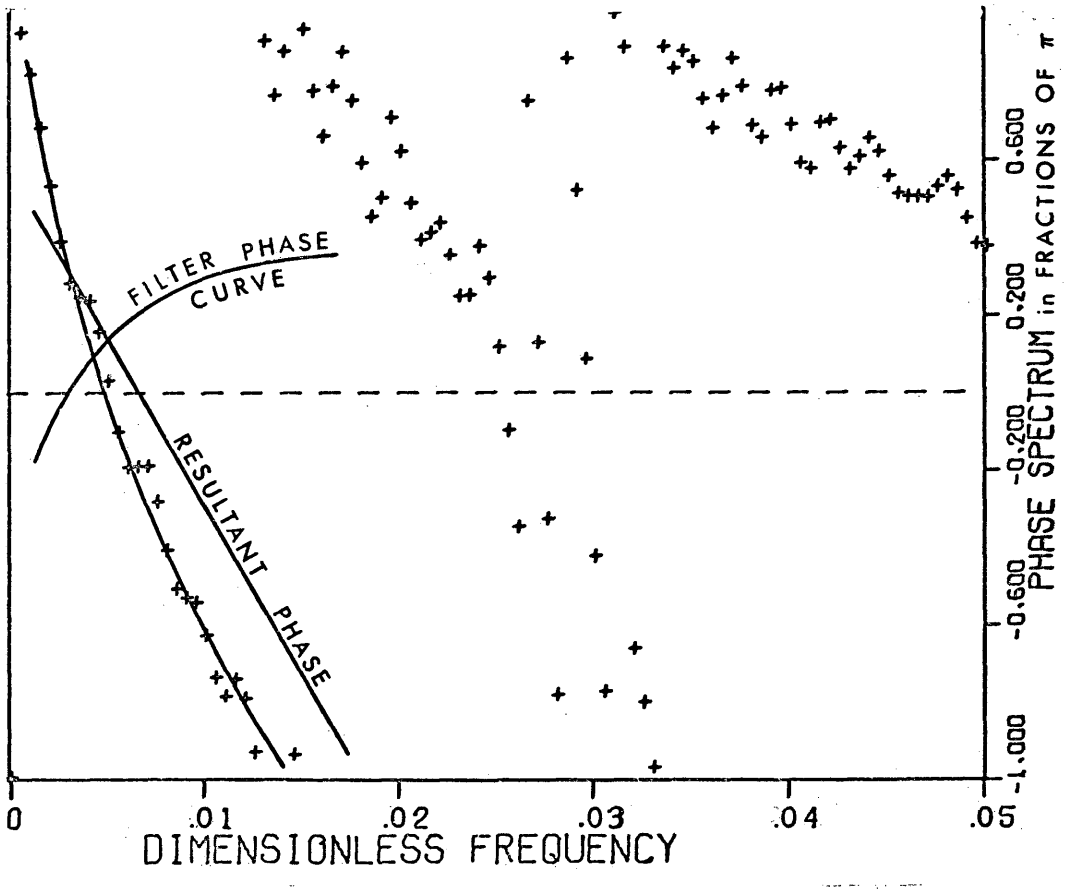

Figure 7 Resultant Phase Spectrum of the Data

We can now proceed to calculate the delay time. Because the frequency axis is dimensionless, $f\Delta T$, we can write

$$\omega t_o = \left(\frac{2\pi t_o}{\Delta t}\right) f\Delta t = mf\Delta t \ .$$

The slope as measured from the graph is

$$m = \frac{-\pi x 10^2}{1.125} \ ,$$

from which we arrive at

$$t_o = -89 \pm 1 \text{ sec.}$$

The result shows that the step component of the propagating elastic disturbance had a delay of 89 seconds with respect to the arbitrary zero time. It is interesting to note that this figure is in close agreement with the apparent delay time of the transient on the filtered record as well as the delay of the recovered strain step shown in Figure 16. This technique for determining t_o seems preferable to the graphic method used by Wideman (1967).

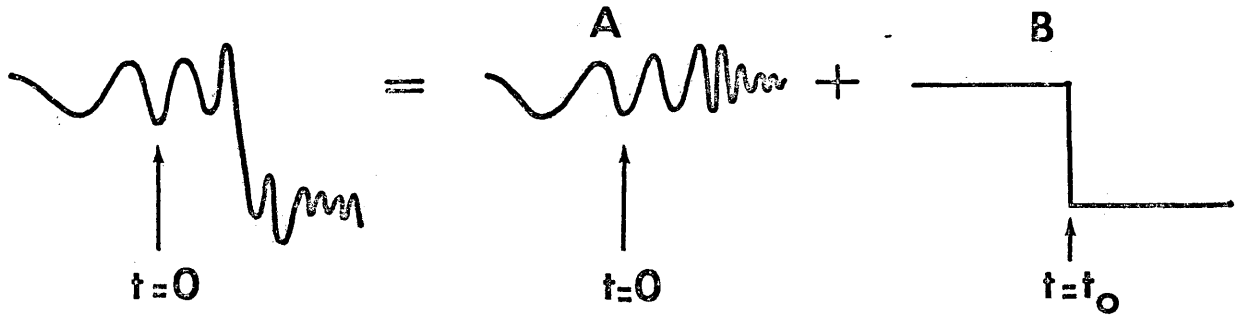

Figure 8. A Simulated Propagating Elastic Disturbance.

INVERSE FILTERING OF THE DATA

The term inverse filtering often refers to an effort to restore attenuated high-frequency components in order to attain improved resolution or pulse compression. In this study such an effort would be blocked by the presence of large amounts of high-frequency energy which are associated with classical body and surface waves as envisioned without permanent changes in strain. Since we wish to study such permanent effects, the classical waves are called noise, and the inverse filter is designed not for pulse compression but rather for pulse expansion.

The process of inverse filtering consisted of three steps: (1) an appropriate inverse filter was designed in the frequency domain, (2) its time-domain equivalent, or the operator, was determined, and (3) the operator was convolved with the sampled data. This section is discussed under the headings listed below:

Design of the Operator

Processing of the Data

Design of the Operator

A cursory review of the frequency response of the recording system (Figure 3) reveals the essential ingredients that the inverse filter should possess. The surface waves, after

being attenuated by at least 34 db, still show an appreciable amount of energy on the filtered record. Therefore, if we are to see anything at all in the processed output other than Rayleigh waves, the inverse filter ought to discriminate against them rather severely. It is obvious that by doing so the high frequencies of anything like component B of Figure 8 will be greatly attenuated. The sacrifice is inevitable; however, the consequences are tolerable. Figure 9, which shows the Fourier transform of a step, clarifies the point. The amplitudes of the high frequencies are relatively small compared to those of lower frequencies.

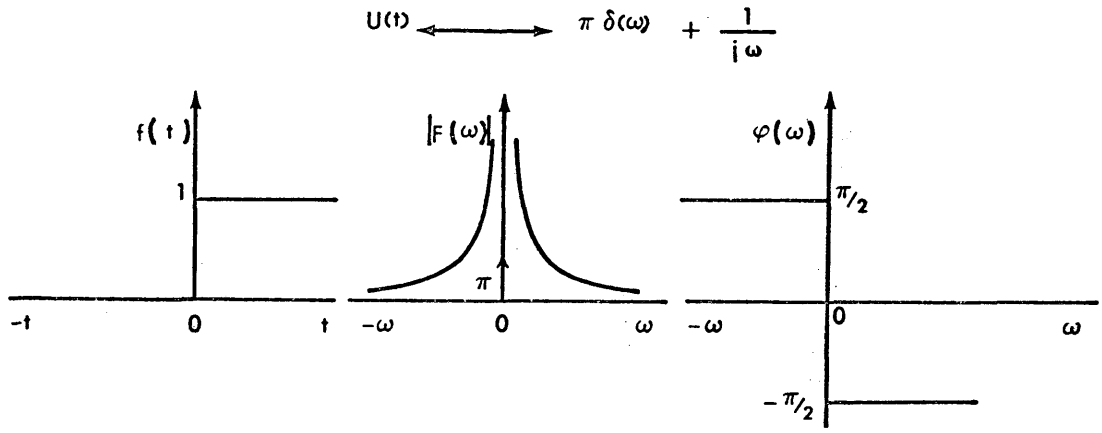

Figure 9. Fourier Transform of a Step.

As a second capability the inverse filter should be able to recover the very low frequencies which were attenuated

by the RC filter. Finally, the filter should compensate for the phase distortion caused by the RC filter.

Figures 10 and 11 show the amplitude and phase of the selected inverse filter. Its system function is

$$W^{-1}(s) = \frac{5\times10^{-2}(S+2\times10^{-3})^2}{(S+10^{-4})^2(S+10^{-1})^2} \quad , \qquad \text{eq. 2}$$

and the corresponding pole-zero diagram is shown in Figure 12.

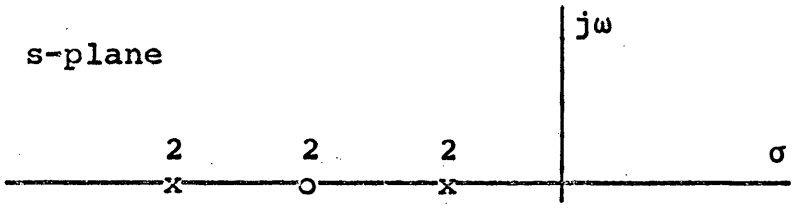

Figure 12. Pole-Zero Diagram of the Operator.

The performance of the operator is summarized below:

1- Attenuates the surface waves for periods smaller than 31 seconds with a cutoff slope of 40 db/decade.
2- Enhances the amplitudes in the period band T = 120 seconds to T = 90,000 seconds to their original unfiltered level to within 10 db (see Figure 13).
3- Compensates the phase in the period band T = 570 seconds to T = 31400 seconds to within 45 degrees (see Figure 14).

The operator is also stable. This follows from the fact that all the poles of the system function are located

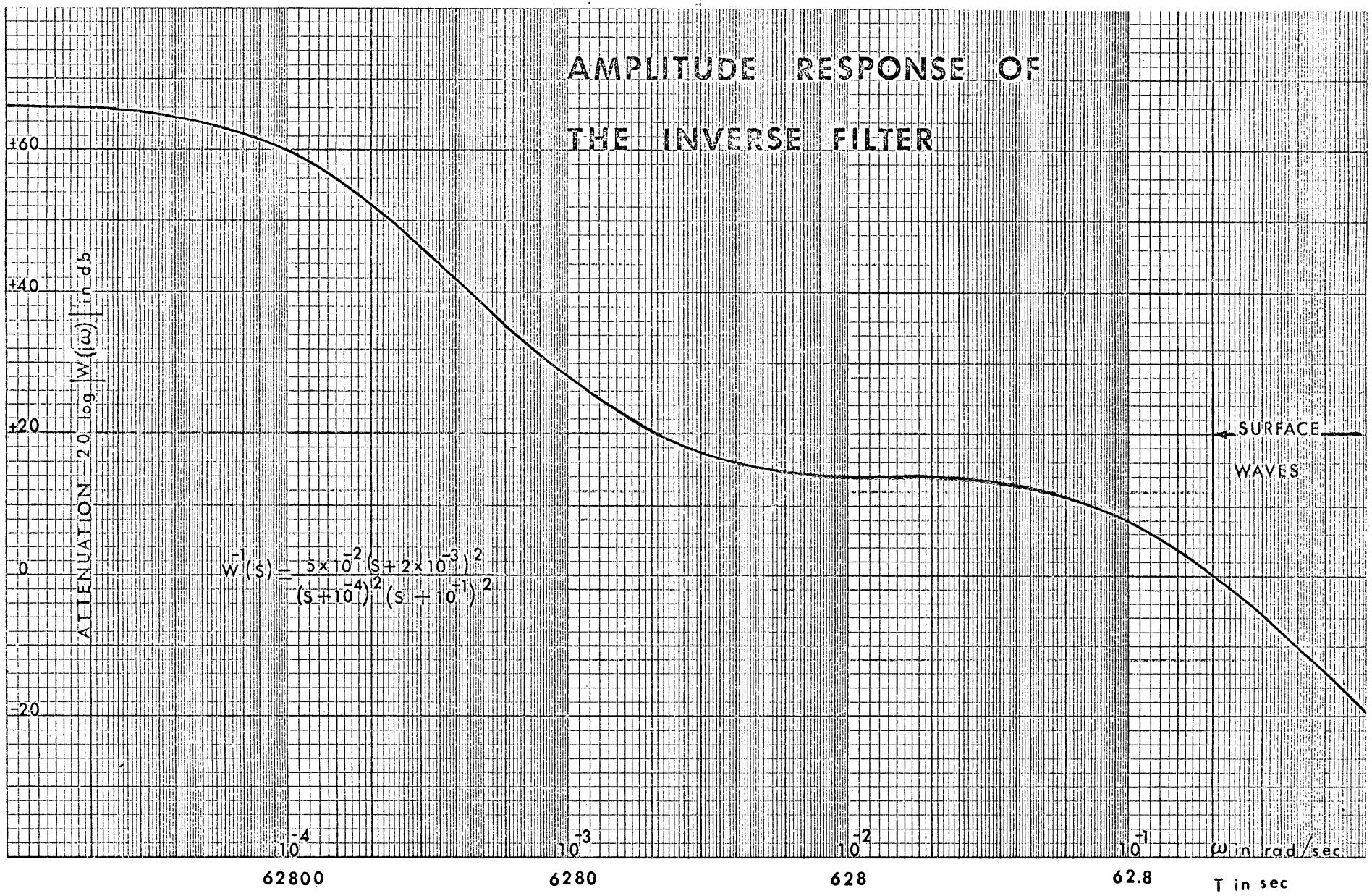
AMPLITUDE RESPONSE OF
THE INVERSE FILTER
+60
+40
+20
0
-20
ATTENUATION = 20 log |W(iω)| in db
$W^{-1}(S) = \frac{5\times10^{-2}(S+2\times10^{-3})^2}{(S+10^{-4})^2(S+10^{-1})^2}$
SURFACE
WAVES
10^{-4}
10^{-3}
10^{-2}
10^{-1}
ω in rad/sec
62800
6280
628
62.8
T in sec

Figure 10

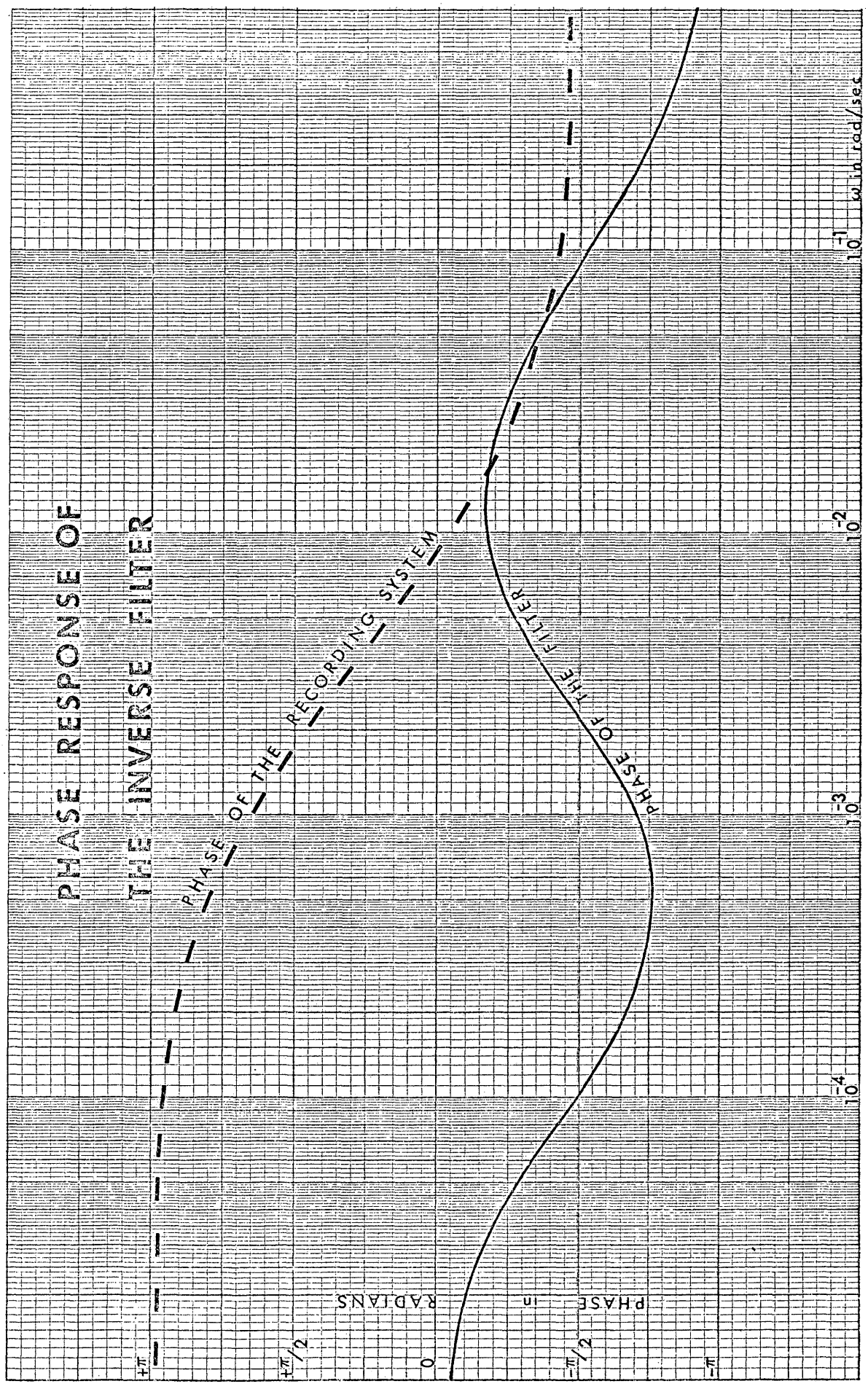
PHASE RESPONSE OF THE INVERSE FILTER
PHASE OF THE RECORDING SYSTEM
PHASE OF THE FILTER
+π
±π/2
0
-π/2
-π
RADIANS
PHASE in
62800
6280
628
62.8
T in sec
10^-4
10^-3
10^-2
10^-1
ω in rad/sec

Figure 11

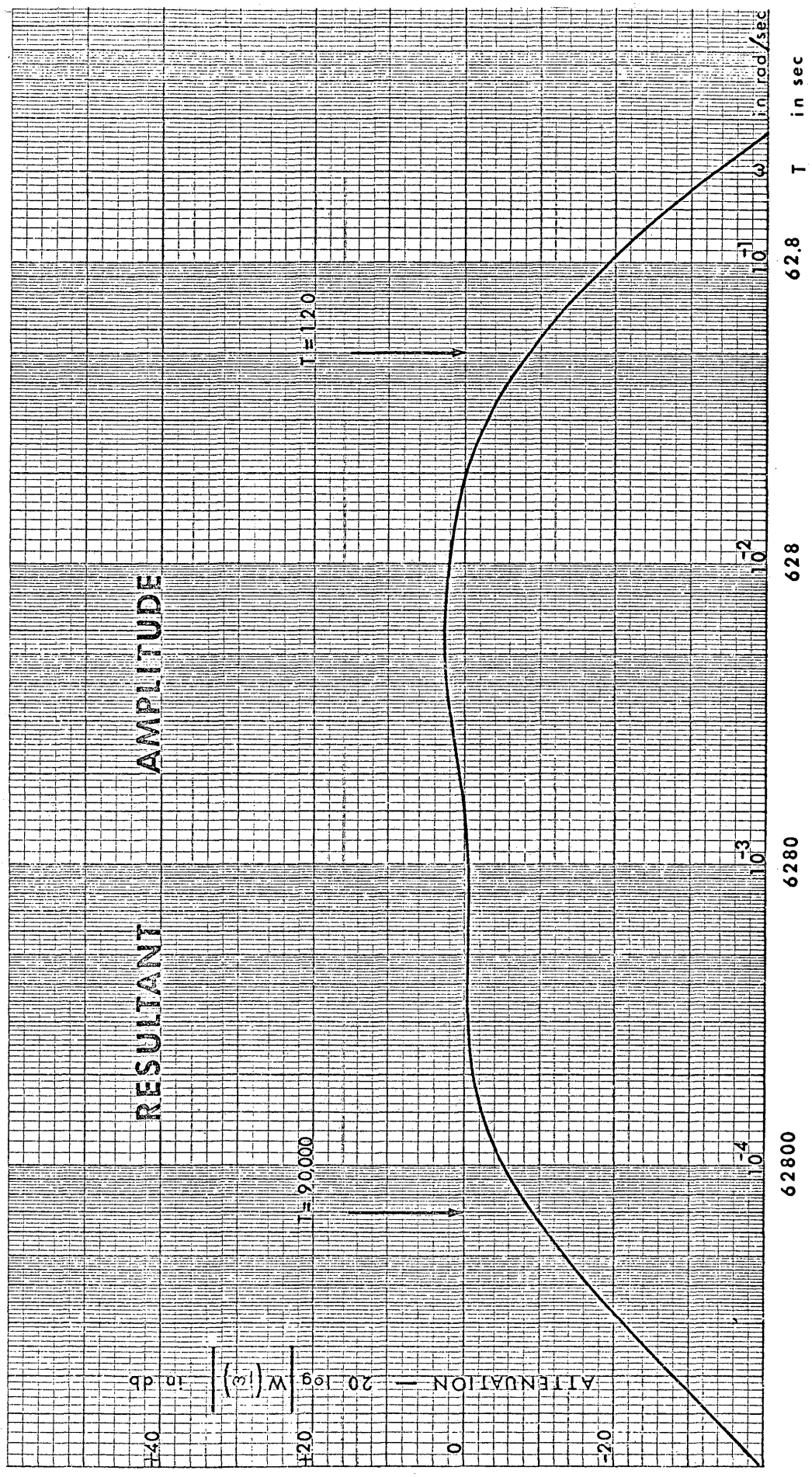
RESULTANT AMPLITUDE
ATTENUATION — 20 log |W(jω)| in db
+40
+20
0
-20
T = 90.000
T = 1.20
62800
6280
628
62.8
10^-4
10^-3
10^-2
10^-1
ω in rad/sec
T in sec

Figure 13

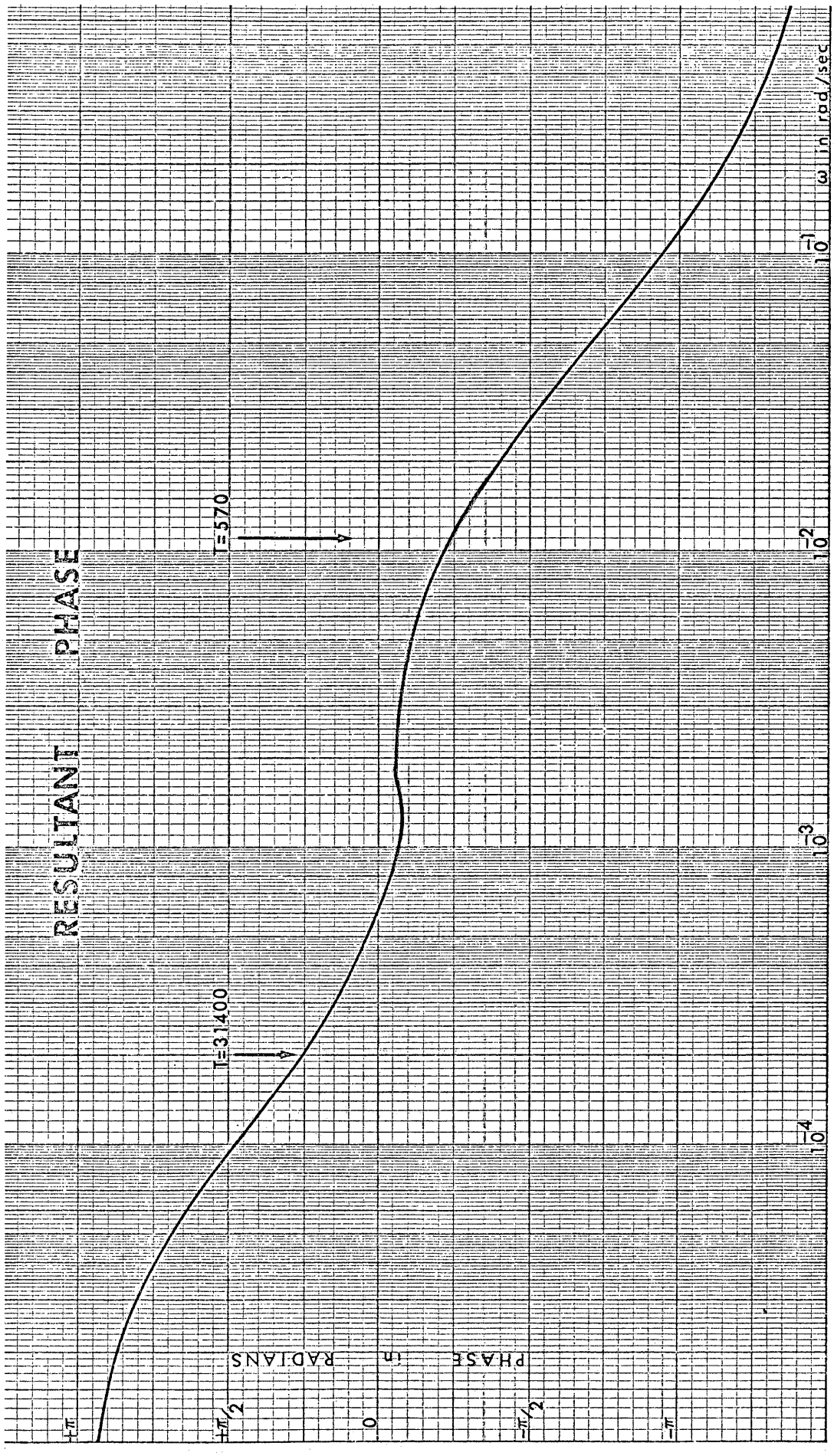
RESULTANT PHASE
PHASE in RADIANS
+π
+π/2
0
-π/2
-π
T=31400
T=570
62800
6280
628
62.8
10^-4
10^-3
10^-2
10^-1
ω in rad./sec
T in sec

Figure 14

on the left-hand side of the S-plane (Aseltine, 1958, p. 137). Therefore,

$$\lim_{t\to\infty} \omega^{-1}(t) = 0.$$

The time-domain equivalent of the filter was obtained by inversion of $W^{-1}(s)$. Hadsell (1968, p. 164) gives the inversion for a system with only real poles as

$$\mathcal{L}^{-1}W^{-1}(s) = \omega^{-1}(t) = \sum_{m=1}^{R} \sum_{k=1}^{\alpha_m} a_{-k}^{m} \frac{t^{k-1}}{(k-1)!} e^{P_m t}$$

where R is the number of real poles, α_m the order of the mth pole, P_m the position of the mth pole, and a_{-k}^{m} are the Laurent coefficients which are

$$a_{-k}^{m} = \frac{1}{(\alpha_m - k)!} \left[\frac{d^{\alpha_m - k}}{ds^{\alpha_m - k}} (s-P_m)^{\alpha_m} W^{-1}(s) \right]_{s=P_m} .$$

By use of the above relations, the inverse of $W^{-1}(s)$ was determined as

$$w^{-1}(t) = (A+Bt)\cdot e^{-t\cdot 10^{-4}} + (C+Dt)\cdot e^{-t\cdot 10^{-1}}$$

where

$$A = 1.9 \times 10^{-2}$$

$$B = 1.8 \times 10^{-5}$$

$$C = -2 \times 10^{-2}$$

$$D = 4.8 \times 10^{-2} .$$

The operator is shown in Figure 15.

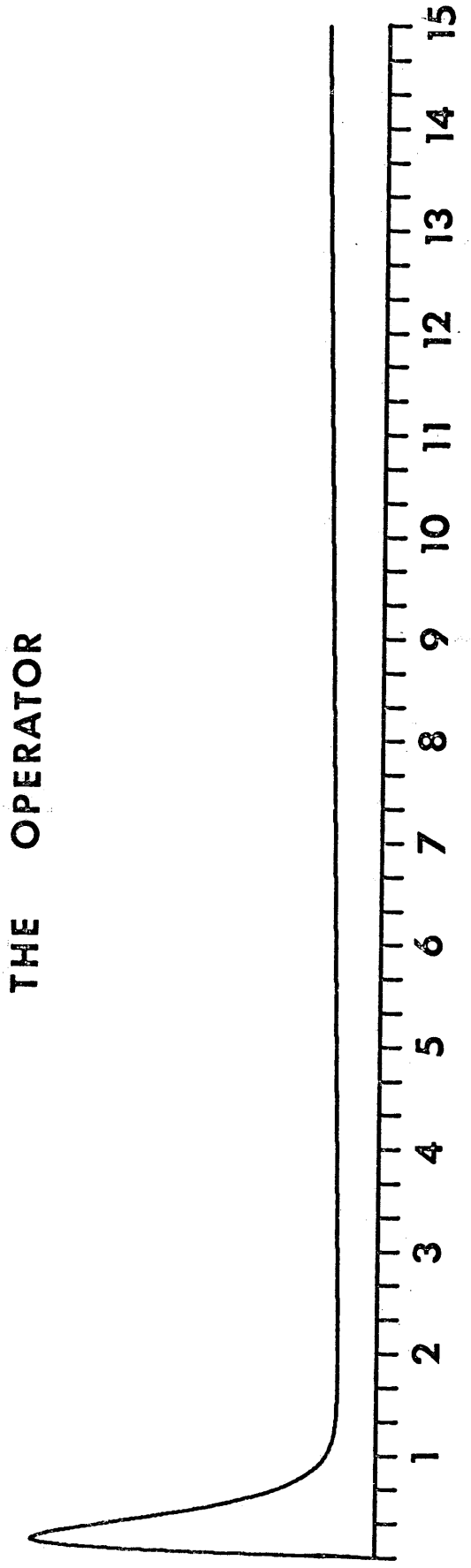

Figure 15

Processing of the Data

In digital processing the word filtering refers to convolution defined as

$$f_1(t)*f_2(t) = \int_{-\infty}^{\infty} f_1(\tau) f_2(t-\tau) d\tau$$

where $f_1(t)$ may be the data and $f_2(t)$ the filter. The transform of this operation is

$$W_1(j\omega) \cdot W_2(j\omega) = A_1(\omega) \cdot A_2(\omega) e^{j\{\phi_1(\omega)+\phi_2(\omega)\}} .$$

It is evident that the product of amplitudes and the addition of phase is the ultimate objective in this endeavour.

Inasmuch as the data were sampled at 2-second intervals, the operator was also sampled at the same rate (program number 3). The operator was then convolved with the sampled data (program number 4). The outcome of the convolution is shown in Figure 16.

The graph is self explanatory. The first 13 minutes of an approximate strain step were recovered from the transient signal. The onset events are clearly Rayleigh waves which reveal a dispersive wave train with an average period of 30 seconds. The step arrives about 90 seconds after the zero time, a close check with the previously computed arrival time. Here, instead of an abrupt step, a rise time of about 30 seconds has been recovered. The reason is obvious if we recall that the operator discriminated

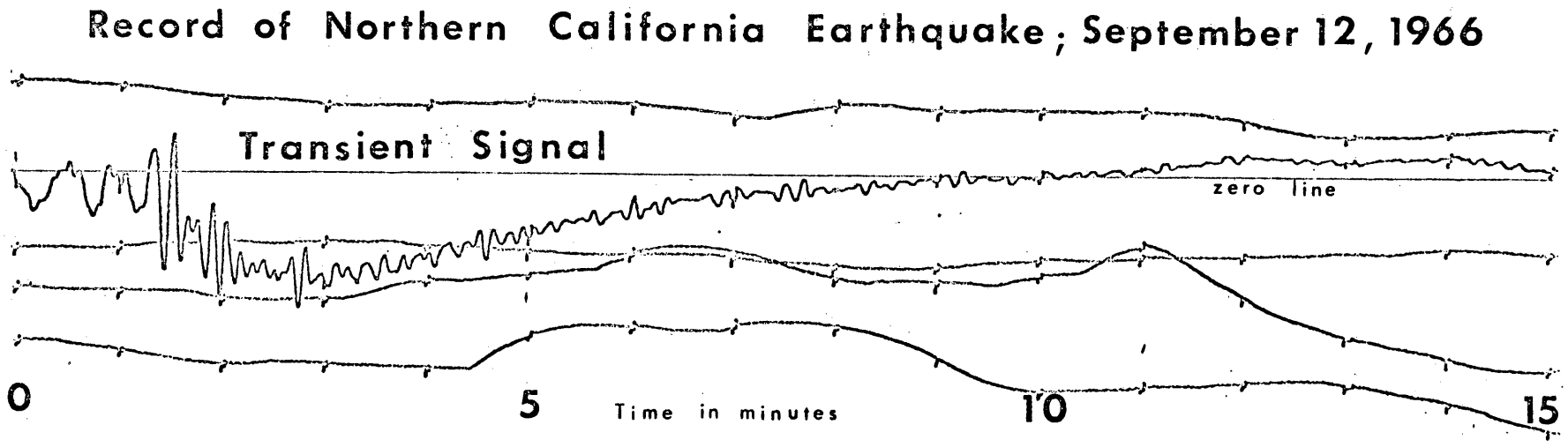
Record of Northern California Earthquake; September 12, 1966
Transient Signal
zero line
0
5
Time in minutes
10
15

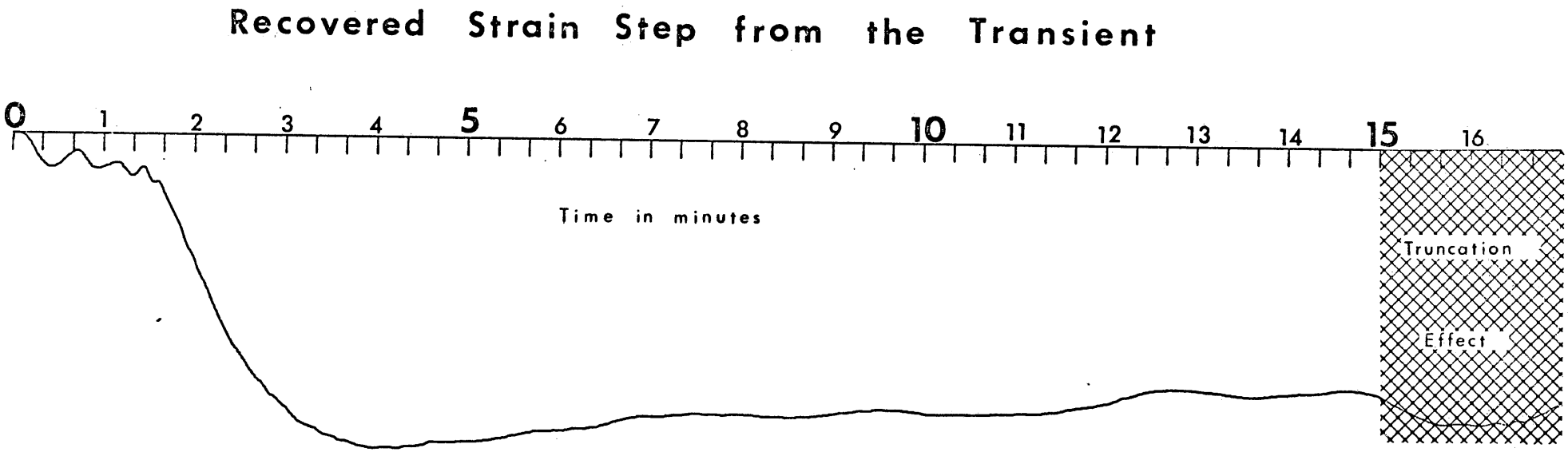
Recovered Strain Step from the Transient
0 1 2 3 4 5 6 7 8 9 10 11 12 13 14 15 16
Time in minutes
Truncation
Effect

Figure 16

against the relatively high frequencies.

There are few other features worth noticing. The low-frequency event arriving at 12 minutes and 40 seconds is believed to be noise. And finally the apparent rise time after 15 minutes is an artifice of data processing. Because the data and filter both had a duration of 15 minutes, this was a truncation effect.

CONCLUSIONS

The reality of permanent strain steps at large epicentral distances has been strongly implied in this paper. By a logical process, which was predominantly deductive, an inverse operator was designed to filter a transient record. The design was based on a knowledge of noise (for the most part crustal waves) and the signal (low-frequency spectrum). The contributions of this paper are summarized below:

An approximate low-pass strain step was recovered from a transient record. The primary uncertainty is due to low-frequency noise (eg., meteorological) which accounts for the ambient or background strain.

From the phase information of the Fourier transform of the data, the arrival time of the strain step was computed.

A measure of the amplitude of the strain step can be obtained if the calibration factor of the strain meter is known.

REFERENCES CITED

Aseltine, John A., 1958, Transform methods in linear system analysis: New York, McGraw-Hill Book Company, Inc., 300 p.

Benioff, Hugo, 1963, Source wave forms of three earthquakes: Seis. Soc. Am. Bull., v. 53, no. 5, p. 893-940.

Gray, Russell L., 1965, The elements of linear filter theory: Golden, Colorado, Colorado School Mines, Department of Geophysics, 145 p.

Hadsell, Frank, 1968, An introduction to the theory of linear data processing: Golden, Colorado, Colorado School Mines Foundation, Inc., 221 p.

Major, Maurice W., Sutton, George H., Oliver, Jack, and Metsger, Robert, 1964, On elastic strain of the earth in the period range 5 seconds to 100 hours: Seis. Soc. Am. Bull., v. 54, no. 1, p. 295-346.

Major, Maurice W., 1966, Residual strain over large areas: ESSA symposium on earthquake prediction, p. 31-37.

Papoulis, A., 1962, The Fourier integral and its applications: New York, McGraw-Hill Book Company, Inc., 318 p.

Pekeris, C. L., 1955, The seismic surface pulse: Natl. Acad. Sci. Proc., v. 41, p. 469-480.

Pipes, L. A., 1958, Applied mathematics for engineers and physicists: New York, McGraw-Hill Book Company, Inc., 723 p.

Press, Frank, 1965, Displacements, strains, and tilts at teleseismic distances: Jour. Geophys. Res., v. 70, no. 10, p. 2395-2412.

Wideman, Charles, 1967, Strain steps associated with earthquakes: Golden, Colorado, Colorado School Mines, MS Thesis 1111, 36 p.